

A CoNi telluride heterostructure supported on Ni foam as an efficient electrocatalyst for oxygen evolution reaction

*Yu Qi,^a Zhi Yang,^a Youcong Dong,^a Xiao-Qing Bao,^b Jilin Bai,^a Hong Li,^a Mitang Wang^c and Dehua Xiong**

- a. State Key Laboratory of Silicate Materials for Architectures, Wuhan University of Technology, Wuhan 430070, P. R. China.
- b. State Key Laboratory of Optical Technologies on Nanofabrication and Microengineering, Institute of Optics and Electronics, Chinese Academy of Sciences, Chengdu 610209, P. R. China.
- c. School of Materials and Chemistry, University of Shanghai for Science and Technology, Shanghai 200093, P. R. China.

* Corresponding author email: xiongdehua2010@gmail.com

List of contents:

Experimental details..... S3-S6

Supplementary figures..... S7-S11

 Fig. S1.....S7

 Fig. S2.....S7

 Fig. S3.....S8

 Fig. S4.....S8

 Fig. S5.....S9

 Fig. S6.....S9

 Fig. S7.....S10

 Fig. S8.....S10

 Fig. S9.....S11

Supplementary Tables.....S12-S14

 Table S1.....S12

 Table S2.....S13

 Table S3.....S14

References.....S15-S16

Experimental details:

Reagents

Sodium tellurite (Na_2TeO_3), Cobalt Nitrate hexahydrate ($\text{Co}(\text{NO}_3)_2 \cdot 6\text{H}_2\text{O}$), hydrazine hydrate ($\text{N}_2\text{H}_4 \cdot \text{H}_2\text{O}$), Potassium hydroxide (KOH), and Ni foam (a thickness of 1.0 mm). All chemicals used are of analytical grade without further purification. Ultrapure deionized (DI) water was used throughout this study.

Preparation of Ni-Te-180C, $\text{Co}(\text{OH})_2@ \text{CoTe}$ -180C, CoNi LDH-180C and CoNi LDH@Te electrodes

Prior to the synthesis, the Ni foam (i. e. $3.0 \times 4.0 \text{ cm}^2$) was soaked in dilute hydrochloric acid (1.0 M HCl) for 30 min to remove the oxide layer on the surface, which made the sample adhere to the surface of Ni foam, and then ultrasonically cleaned in deionized (DI) water and absolute ethanol for 30 min. and finally dried at $50 \text{ }^\circ\text{C}$ in vacuum for 6 hours. The self-supporting electrode was synthesized by a simple one-step hydrothermal method. In the typical synthesis, 0.444 g Na_2TeO_3 and 0.40 g $\text{Co}(\text{NO}_3)_2 \cdot 6\text{H}_2\text{O}$ were dissolved in 65.0 ml deionized water to form a homogeneous solution, and then slowly adding 5.0 ml of $\text{N}_2\text{H}_4 \cdot \text{H}_2\text{O}$, continue to stir the solution for 30 min. The pretreated Ni foam was immersed in a 100 ml Teflon-lined autoclave reactor containing the above mixed solution. Subsequently, the autoclave reactor was sealed, heated to $180 \text{ }^\circ\text{C}$ and maintained 20 hours for hydrothermal reaction. Lastly, washing with deionized water and absolute ethanol for 30 min and drying at $60 \text{ }^\circ\text{C}$ for 6 hours (denoted as 0.4CoNi LDH@Te-180C). By changing the amount of $\text{Co}(\text{NO}_3)_2 \cdot 6\text{H}_2\text{O}$ (0.10 g, 0.20 g, 0.30 g and 0.40 g) under the same conditions, we can get the samples (hereafter denoted as 0.1CoNi LDH@Te-180C, 0.10 g; 0.2CoNi LDH@Te-180C, 0.20 g; 0.3CoNi LDH@Te-180C, 0.30 g and 0.4CoNi LDH@Te-180C, 0.40 g). Furtherly, we change the hydrothermal reaction temperature to $160 \text{ }^\circ\text{C}$, $180 \text{ }^\circ\text{C}$ and $200 \text{ }^\circ\text{C}$ comparative study (denoted as 0.4CoNi LDH@Te-160C, $160 \text{ }^\circ\text{C}$; 0.4CoNi LDH@Te-180C, $180 \text{ }^\circ\text{C}$ and 0.4CoNi LDH@Te-200C, $200 \text{ }^\circ\text{C}$). When the Ni foam was telluride, the obtained electrode was recorded as Ni-Te-180C; when the Ni foam is not added, the sample is marked as $\text{Co}(\text{OH})_2@ \text{CoTe}$ -180C; when Na_2TeO_3 was

not introduced into the solution, the obtained electrode was recorded as CoNi LDH-180C.

Structural characterization

The morphology, microstructure, and chemical composition of bare Ni foam (denoted as bare NF), Ni-Te-180C, Co(OH)₂@CoTe-180C, CoNi LDH-180C and CoNi LDH@Te electrodes were examined by field-emission scanning electron microscopy (FESEM, FEG Quanta 450) and transmission electron microscopy (TEM, JEOL JEM-2100 operating at 200 keV) equipped with energy-dispersive X-ray spectroscopy (EDS). The mean particle size was detected by a laser granularity meter (Malvern M3600), operating with laser diffraction and previous ultrasonication of the synthesized 0.4CoNi LDH@Te-180C in deionized water. An atomic force microscopy (AFM) with DI Nanoscope IV controller (Veeco, USA) was used to record the AFM height images of all these samples. The elements content of Ni, Co and Te was quantified analysis by an inductively coupled plasma-optical emission spectrometry (ICP-OES, Prodigy 7). The crystalline structure of samples was studied by X-ray diffractometry (XRD, PANalytical X'Pert PRO) using Cu K α radiation ($\lambda = 1.540598 \text{ \AA}$) and a PIXcel detector. The surface chemical states of 0.4CoNi LDH@Te-180C were analyzed by X-ray photoelectron spectroscopy (XPS, Thermo Escalab 250 Xi), and the C (1s) line (at 284.80 eV) corresponding to the surface adventitious carbon (C-C line bond) has been used as the reference binding energy.

Electrochemical measurements

The OER performance was evaluated by cyclic voltammetry (CV), chronopotentiometry (CP) and electrochemical impedance spectroscopy (EIS) in a three-electrode configuration in 1.0 M KOH (pH = 13.5) using a CS2350H electrochemical workstation (Wuhan Corrtest Instruments Corp., China). A platinum wire and a saturated calomel electrode (SCE) were used as the counter and reference electrodes, respectively. The as-fabricated 0.4CoNi LDH@Te-180C working electrode was directly used as the working electrode, and the active electrode area was kept to $1.0 \times 1.0 \text{ cm}^2$. Cyclic voltammetric (CV) scans were recorded between 1.05 and 1.80

V vs. reversible hydrogen electrode (RHE) at the scan rate of 5 mV s⁻¹. The electrochemical double-layer capacitance (C_{dl}) of each sample was measured given that C_{dl} is positively proportional to the effective surface areas (ESA). C_{dl} can be extracted through CV scans at different rates (from 10 to 100 mV s⁻¹) in the non-faradaic potential window of -0.05 - 0.05 V vs. SCE. All current density values were normalized with respect to the geometrical surface area of the working electrode. For comparison, the electrocatalytic performance of a bare NF and Ni-Te-180C was also measured. All CV curves presented in this work are iR-corrected (85%), and the correction was done according to the following equation:

$$E_c = E_m - iR_s \quad (1)$$

where E_c is the iR-corrected potential, E_m experimentally measured potential, and R_s the equivalent series resistance extracted from the electrochemical impedance spectroscopy (EIS) measurements. Unless otherwise specified, all potentials are reported versus reversible hydrogen electrode (RHE) by converting the potentials measured vs. SCE according to the following formula:

$$E(\text{RHE}) = E(\text{SCE}) + 0.241 + 0.059 \text{ pH} \quad (2)$$

The EIS measurements were performed in the frequency range of 10 mHz - 100 kHz under a constant potential of 1.60 V vs. RHE.

The Turnover frequency (TOF_{mass}) values were calculated through the following equation:

$$\text{TOF} (\text{s}^{-1}) = (j \times A) / (4 \times F \times n) \quad (3)$$

where j (A cm⁻²) is the current density at a given overpotential, $A = 1.0$ cm² is the geometric surface area of the working electrode, $F = 96500$ C mol⁻¹ stands for the Faraday constant, n (mol) is mole number of active catalyst loaded on the electrode.

To estimate the Faradic efficiency of 0.4CoNi LDH@Te-180C catalyst, a galvanostatic catalysis was carried out at 20 mA cm⁻² for 60 min. Before test, the 1.0 M KOH electrolyte was degassed by argon gas for 30 min. The quantities of the generated H₂ and O₂ were determined every 10 min by an Agilent 8860 gas

chromatography.

The Faraday efficiency was calculated by the following equation:

$$FE = \frac{L \times N \times F}{V_m \times t \times i} \times 100\% \quad (4)$$

Where t is the reaction time (s), i is the test current (A), N (=2 or 4) is the number of electrons transferred to form H₂ or O₂ molecules, F is the Faraday constant (96485 C mol⁻¹), L is the volume of H₂ or O₂ gas actually produced (L); V_m is the molar volume of gas at room temperature of 25 °C (L mol⁻¹).

Supplementary figures:

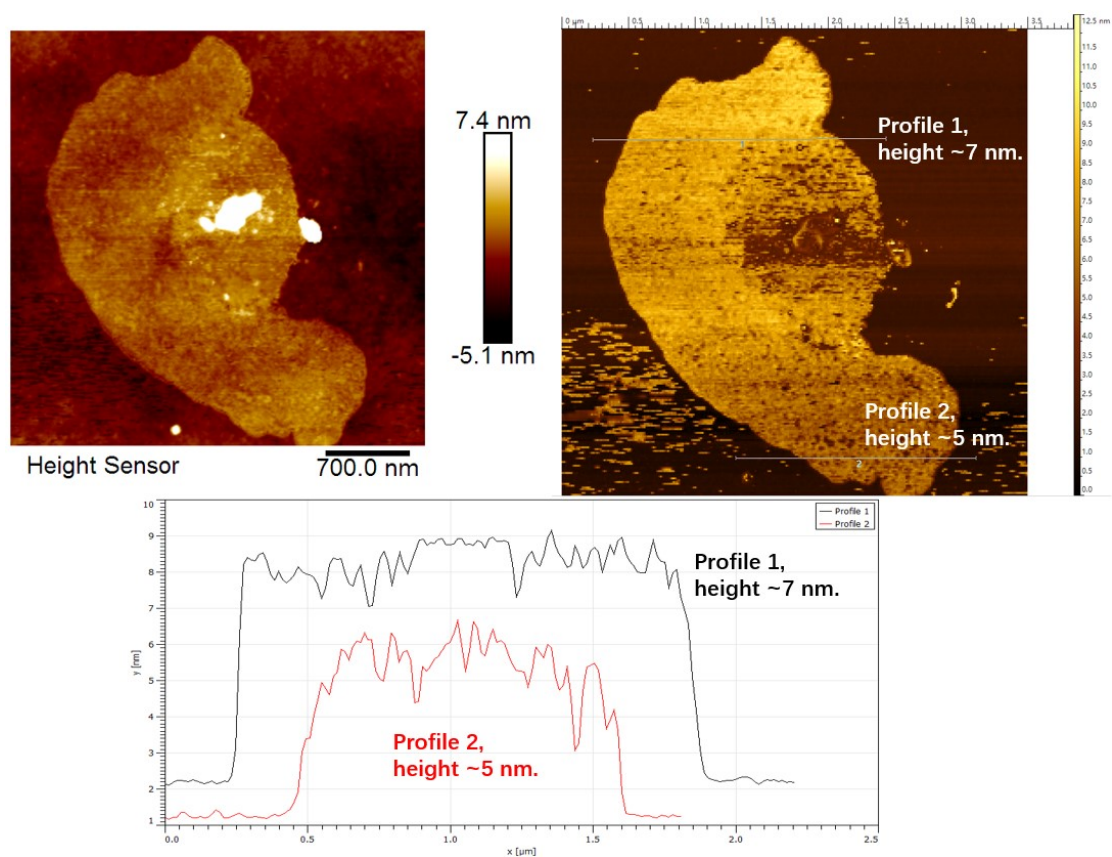


Fig. S1 AFM image and curve diagram showing thickness distribution of 0.4CoNi LDH@Te-180C

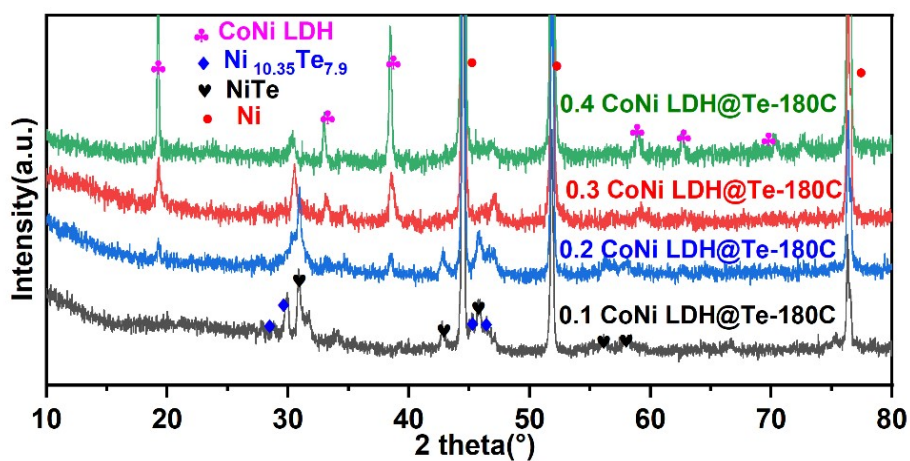


Fig. S2 XRD pattern of 0.1CoNi LDH@Te-180C, 0.2CoNi LDH@Te-180C, 0.3CoNi LDH@Te-180C and 0.4CoNi LDH@Te-180C samples.

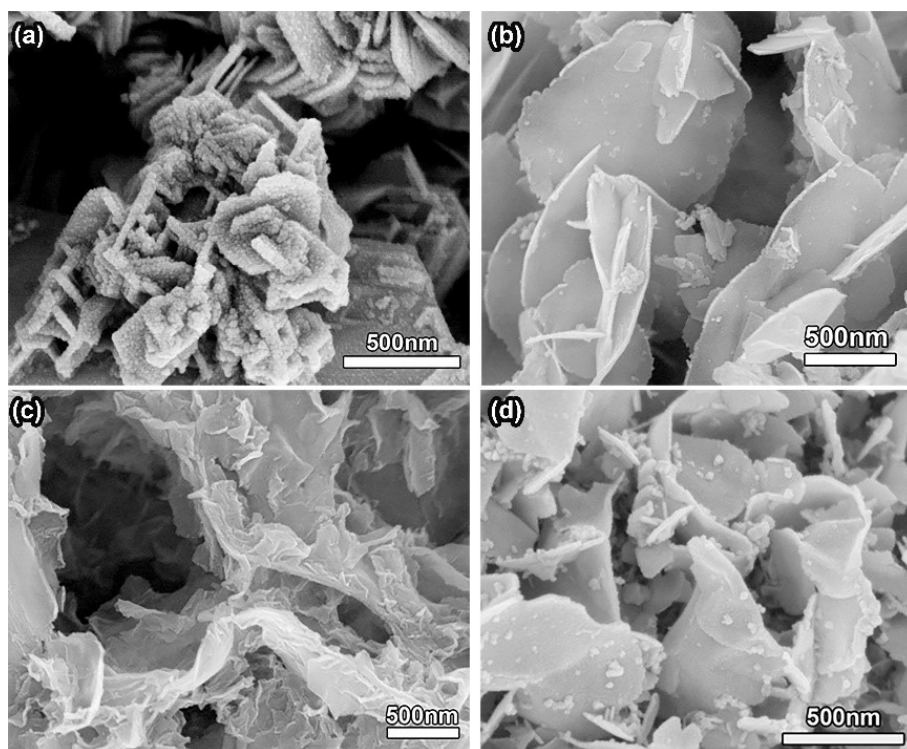


Fig. S3 SEM mages of 0.1CoNi LDH@Te-180C, 0.2CoNi LDH@Te-180C, 0.3CoNi LDH@Te-180C and 0.4CoNi LDH@Te-180C samples.

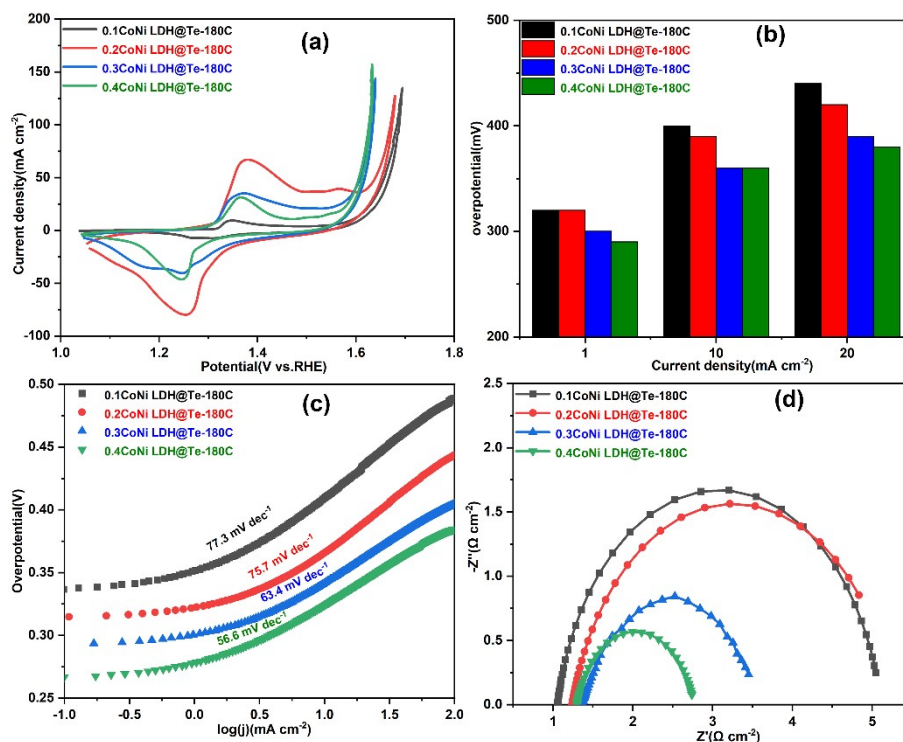


Fig. S4 (a) CV curves, (b) the overpotentials needed to achieve different anodic current densities, (c) Tafel plots and (d) Nyquist plots of 0.1CoNi LDH@Te-180C, 0.2CoNi LDH@Te-180C, 0.3CoNi LDH@Te-180C and 0.4CoNi LDH@Te-180C samples.

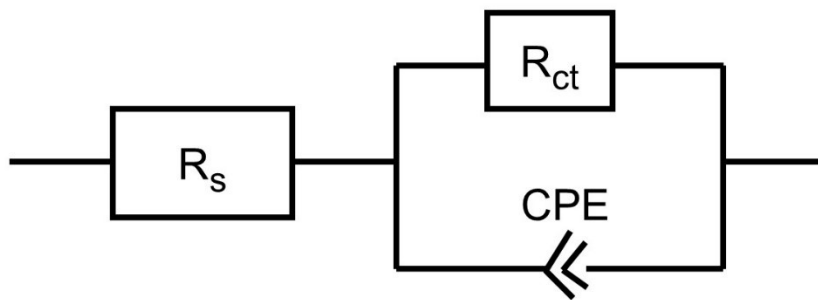


Fig. S5 Equivalent circuit models of bare NF, Ni-Te-180C and 0.4CoNi LDH@Te-180C samples used for EIS fitting

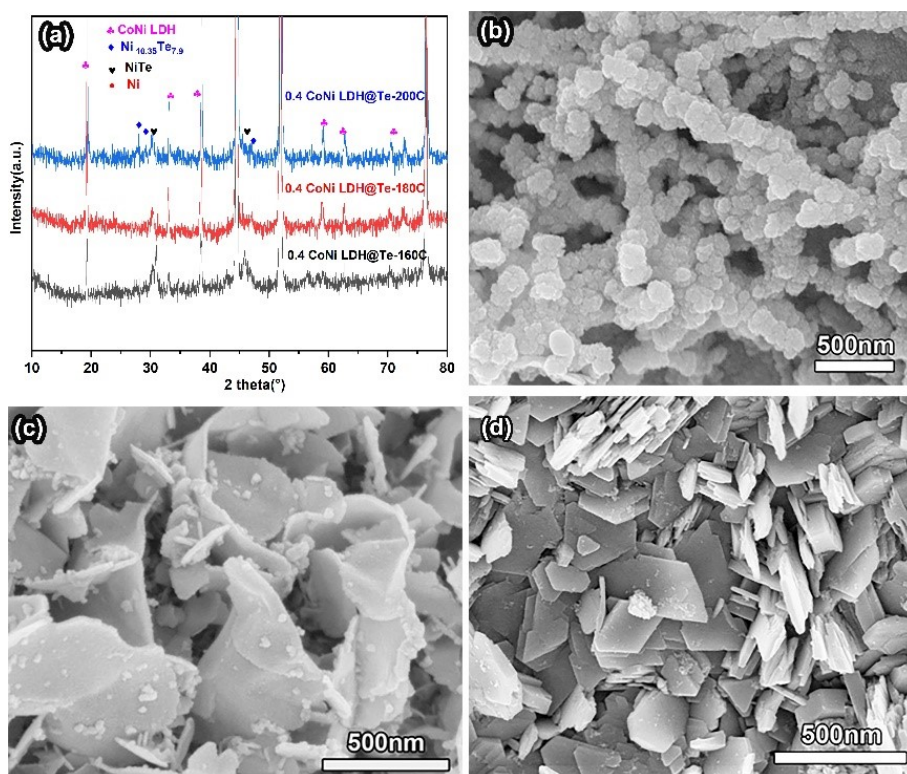


Fig. S6 (a) XRD pattern of 0.4CoNi LDH@Te-160C, 0.4CoNi LDH@Te-180C, and 0.4CoNi LDH@Te-200C; (b-d) the SEM images of 0.4CoNi LDH@Te-160C, 0.4CoNi LDH@Te-180C, and 0.4CoNi LDH@Te-200C samples.

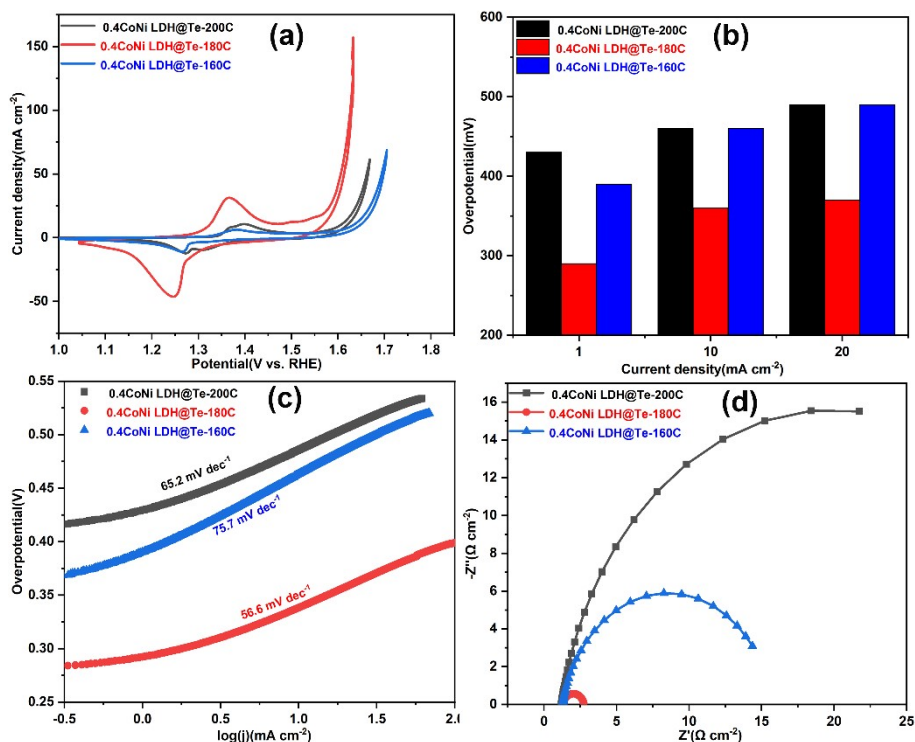


Fig. S7 (a) CV curves, (b) Tafel plots, (c) Nyquist plots and (d) current density ($J = 0.5 \times (J_a - J_c)$) as a function of scan rates of 0.4CoNi LDH@Te-160C, 0.4CoNi LDH@Te-180C, and 0.4CoNi LDH@Te-200C samples.

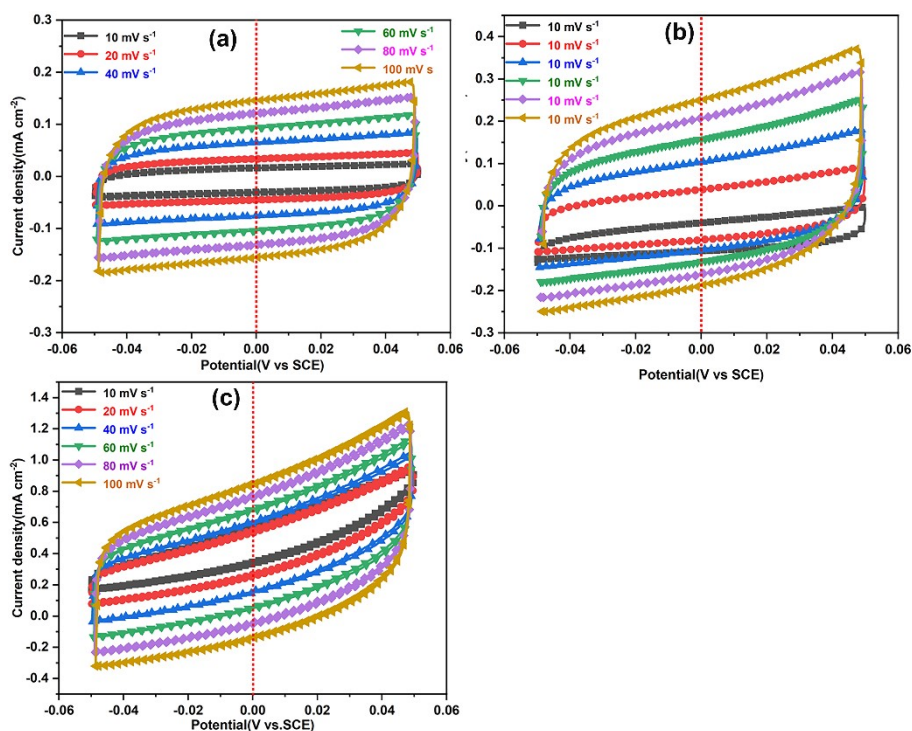


Fig.S8 CV curves (a-c) of the bare NF, Ni-Te-180C and 0.4CoNi LDH@Te-180C electrodes measured in 1.0 M KOH in the non-faradaic region at different scan rates ranging from 10 to 100 mV s^{-1} .

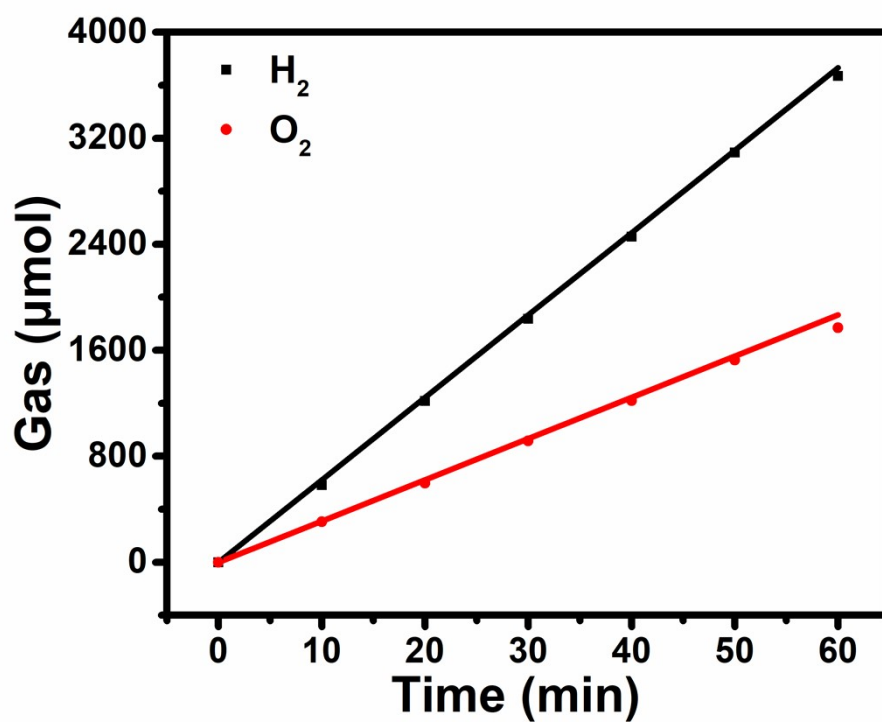


Fig. S9 Experimental and theoretical calculated amounts of gas from the OER of 0.4CoNi LDH@Te-180C electrode at a current density of 20 mA cm⁻² for Faradaic efficiency calculation.

Supplementary Tables:

Table S1 Chemical compositions of 0.4CoNi LDH@Te-180C and 0.4CoNi LDH@Te-180C-OER based samples deduced from ICP-OES measurements

Samples (at%)	Ni/%	Co/%	Te/%	Total/%
0.4CoNi LDH@Te-180C	96.6	0.3	3.1	100.0
0.4CoNi LDH@Te-180C-OER	97.7	0.3	2.0	100.0

Supplementary information

Table S2 Comparison of electrocatalytic parameters of 0.4CoNi LDH@Te-180C electrodes toward OER

Catalysts	Electrolyte	Tafel slope (mV dec ⁻¹)	J _{geo} (Current density in mA cm ⁻² @overpotential in mV)	Reference
0.4CoNi LDH@Te-180C	1.0 M KOH	56.6	η₁₀ = 360 mV	This work
NiCo-NF	1.0 M KOH	91.0	η ₁₀ = 437 mV	ACS Appl. Energy Mater., 2019, 2, 312-319. ¹
CoNi LDH CoNi LDH@HOS	0.1 M KOH	113.0 72.0	η ₁₀ = 420 mV η ₁₀ = 273 mV	ACS Appl. Energy Mater., 2018, 1, 4040-4049. ²
CoNi LDH	1.0 M KOH	118.0	η ₁₀ = 460 mV	Int. J. Hydrogen Energ., 2020, 45, 12629-12640. ³
CoNi LDH/NF CoNi LDH-P/NF	1.0 M KOH	72.0 242.0	η ₁₀ = 271 mV η ₁₀ = 430 mV	Dalton Trans., 2017, 46, 8372-8376. ⁴
Fe _{6%} /CoNi LDH		46	η ₁₀ = 251 mV	
Fe _{8%} /CoNi LDH	1.0 M KOH	25	η ₁₀ = 232 mV	J. Iran. Chem. Soc., 2020, 17, 2943-2956. ⁵
Fe _{10%} /CoNi LDH		38	η ₁₀ = 242 mV	
0.6Te-CoNi LDH	1.0 M KOH	45.4	η ₁₀ = 290 mV	J. Solid State Electr., 2007, 11, 1355-1364. ⁶
Ni-BDC@NiFe-LDH-2	1.0 M KOH	45	η ₁₀ = 272 mV	CrystEngComm., 2021, 23, 1172-1180. ⁷
NiFe LDH/NiTe	1.0 M KOH	---	η ₅₀ = 228 mV	Appl. Catal. B, 2020, 273, 119014. ⁸
Ni ₃ Te ₂ -CoTe	1.0 M KOH	68	η ₁₀ = 310 mV	Appl. Surf. Sci., 2019, 490, 516-521. ⁹
NiCo-NiCoO ₂ nano-heterostructure	1.0 M KOH	---	η ₁₀ = 327 mV	Int. J. Hydrogen Energ., 2021, 46, 18936-18948. ¹⁰
NiCo-NiCoO ₂ nano-heterostructure	1.0 M KOH	---	η ₁₀ = 266 mV	Journal of Energy Chemistry, 2021, 57, 99-108. ¹¹
Co _{1.8} Ni(OH) _{5.6} @ Co _{1.8} NiS _{0.4} (OH) _{4.8}	0.1 M KOH	45.0	η ₁₀ = 274 mV	Adv. Mater., 2019, 31, 1805658. ¹²
Co _{1.8} Ni(OH) _{5.6}		89.1	η ₁₀ = 390 mV	
Co _{1.8} NiS _{1.6} (OH) _{2.2}		71.2	η ₁₀ = 326 mV	

Supplementary information

Table S3 Estimated compositions in 0.4CoNi LDH@Te-180C catalysts obtained from EDS results.

Catalysts	Ni (at%)	Co (at%)	Te (at%)	O (at%)
0.4CoNi LDH@Te-180C	33.0	2.0	15.0	50.0
0.4CoNi LDH@Te-180C- OER	35.0	3.0	3.0	59.0

References

1. S. Sun, C. Lv, W. Hong, X. Zhou, F. Wu and G. Chen, Dual Tuning of Composition and Nanostructure of Hierarchical Hollow Nanopolyhedra Assembled by NiCo-Layered Double Hydroxide Nanosheets for Efficient Electrocatalytic Oxygen Evolution, *Acs Appl.Energ. Mater.*, 2019, **2**, 312-319.
2. K. Xiang, J. Guo, J. Xu, T. Qu, Y. Zhang, S. Chen, P. Hao, M. Li, M. Xie, X. Guo and W. Ding, Surface Sulfurization of NiCo-Layered Double Hydroxide Nanosheets Enable Superior and Durable Oxygen Evolution Electrocatalysis, *Appl.Energ. Mater.*, 2018, **1**, 4040-4049.
3. S. Wang, T. Wang, X. Wang, Q. Deng, J. Yang, Y. Mao and G. Wang, Intercalation and elimination of carbonate ions of NiCo layered double hydroxide for enhanced oxygen evolution catalysis, *J. Hydrogen Energ.*, 2020, **45**, 12629-12640.
4. W. Liu, J. Bao, M. Guan, Y. Zhao, J. Lian, J. Qiu, L. Xu, Y. Huang, J. Qian and H. Li, Nickel-cobalt-layered double hydroxide nanosheet arrays on Ni foam as a bifunctional electrocatalyst for overall water splitting, *Dalton T.*, 2017, **46**, 8372-8376.
5. A. Parkash, Doping of Fe on room-temperature-synthesized CoNi layered double hydroxide as an excellent bifunctional catalyst in alkaline media, *J. Iran. Chem. Soc.*, 2020, **17**, 2943-2956.
6. J. W. Lee and B. N. Popov, Ruthenium-based electrocatalysts for oxygen reduction reaction-review., *Solid State Electrochem.*, 2007, **11**, 1355-1364.
7. Q. Dong, C. Shuai, Z. Mo, R. Guo, N. Liu, G. Liu, J. Wang, W. Liu, Y. Chen, J. Liu, Y. Jiang and Q. Gao, The in situ derivation of a NiFe-LDH ultra-thin layer on Ni-BDC nanosheets as a boosted electrocatalyst for the oxygen evolution reaction, *CrystEngComm.*, 2021, **23**, 1172-1180.
8. L. Hu, X. Zeng, X. Wei, H. Wang, Y. Wu, W. Gu, L. Shi, and C. Zhu, Interface engineering for enhancing electrocatalytic oxygen evolution of NiFe LDH/NiTe heterostructures, *Appl. Catal. B.*, 2020, **273**, 119014.
9. J. Xu, Y. Q. Yin, H. Q. Xiong, X. D. Du, Y. J. Jiang, W. Guo, Z. Wang, Z. Z. Xie, D. Y. Qu, H. L. Tang, Q. B. Deng and J. S. Li, Improving catalytic activity of metal telluride by hybridization: An efficient Ni₃Te₂-CoTe composite electrocatalyst for oxygen evolution reaction, *Appl. Surf. Sci.*, 2019, **490**, 516-521.

10. U. Y. Qazi, R. Javaid, M. T. Zahid, A. Nadeem and X. M. Lin, Bimetallic NiCo-NiCoO₂ nano-heterostructures embedded on copper foam as a self-supported bifunctional electrode for water oxidation and hydrogen production in alkaline media. *Int. J. Hydrogen Energ.*, 2021, **46**, 18936-18948.
11. Li, Y., Wang, W., Huang, B., Mao, Z., Wang, R., He, B., Gong, Y., Wang, H. Abundant heterointerfaces in MOF-derived hollow CoS₂-MoS₂ nanosheet array electrocatalysts for overall water splitting. *Journal of Energy Chemistry*, 2021, **57**, 99-108.
12. B. Wang, C. Tang, H. F. Wang, X. Chen, R. Cao, and Q. Zhang, A Nanosized CoNi Hydroxide@Hydroxysulfide Core-Shell Heterostructure for Enhanced Oxygen Evolution. *Adv. Mater.*, 2019, **31**, 1805658.